Int J Clin Exp Pathol 2020;13(6):1349-1360
www.ijcep.com /ISSN:1936-2625/IJCEP0110192

*Original Article*

# Hyperplasia suppressor gene inhibits the proliferation and metastasis of glioma cells by targeting rho family proteins

Juncheng Wang[1*], Bin Zhang[2,3*], Haibo Liu[2], Qiao Wu[4], Peng Gao[1,2], Yourui Zou[2], Yanping Lan[1], Qinghua Zhang[5]

*[1]Department of Neurosurgery, People's Hospital of Ningxia Hui Autonomous Region, Yinchuan 750001, Ningxia, China; [2]Department of Neurosurgery, General Hospital of Ningxia Medical University, Yinchuan 750001, Ningxia, China; [3]Ningxia Key Laboratory of Cerebrocranial Diseases, Ningxia Medical University, Yinchuan 750001, Ningxia, China; [4]Department of Neurosurgery, Fuzhou First People's Hospital, Fuzhoou 350000, Fujian, China; [5]Department of Neurosurgery, Xiehe Shenzhen Hospital of Huazhong University of Science and Technology (Nanshan Hospital), Shenzhen 518000, Guangdong, China. [*]Equal contributors.*

Received March 2, 2020; Accepted April 14, 2020; Epub June 1, 2020; Published June 15, 2020

**Abstract:** Aim: To investigate the effect of the hyperplasia suppressor gene (HSG) on human glioma cell invasion and its possible mechanism. Methods: Human glioma U251 cells were infected with recombinant viral vectors carrying the HSG gene sequence (HSG overexpression group) and HSG interference sequence (HSG suppression group). The negative control group with no-load virus transcription and a blank control group with only PBS treatment were set up. CCK-8 assay, cell scratch healing test, transwell migration, and invasion test were used to detect the effect of HSG expression on proliferation, migration and invasion of U251 glioma cells. Cell immunofluorescence and cell adhesion test were used to analyze the effect of HSG expression on cytoskeleton formation and adhesion ability of U251 cells. Gene chip technology was employed to preliminarily explore the effect of HSG expression change on the inherent gene expression in U251 cells. The expression of Rho family key molecule mRNA and protein was detected by light quantitative PCR and western blot. Results: After 24 h of transcription with the recombinant virus vector, the cells showed a green color under an inverted fluorescence microscope. HSG expression increased in the HSG overexpression group ($P < 0.01$), and decreased in the HSG inhibition group ($P < 0.01$). Compared with the two control groups, the proliferation, scratch healing rate, migrating cell number, invasive cell number and adhesion cell number in the HSG overexpression group were markedly lower. After HSG overexpression, the morphology of U251 cells changed; filamentous pseudopods shortened and partially flaked. However, after HSG inhibition, the pseudopods grew toward both ends and were arranged axially. The overexpression of HSG inhibited the expression of rho family proteins (RhoA, Rock1, Rock2, Rac1, and Cdc42). Conclusion: The overexpression of HSG inhibits the progression of glioma U251 cells by regulating the expression of rho family proteins.

**Keywords:** HSG, glioma, proliferation, invasion, Rho protein

## Introduction

Glioma is the most common malignant tumor in the nervous system. Its main feature is the high rate of invasion of peripheral brain tissue. In many patients, many tumor cells have invaded into the normal brain tissue before diagnosis, so that the tumor cannot be removed completely. Although supplemental radiotherapy and chemotherapy are given after surgery, the median survival time of patients is only 16-18 months [1-4]. Therefore, the invasion of glioma cells is the root cause of glioma recurrence [5]. Effective control of the invasion of glioma cells is a key goal in the treatment of glioma.

The hyperplasia suppressor gene (HSG) is related to cell proliferation, as discovered by Chen et al. [6]. In recent years, HSG has been extensively studied in breast cancer, lung cancer, liver cancer, bladder cancer and colon cancer. Previous studies have suggested that exogenous HSG transfection can inhibit the growth of tumor cells and promote apoptosis [7-9], and

the anti-tumor effect of HSG is higher than that of p53 [6]. Moreover, Zhang et al. [10] reported that HSG could inhibit the invasion and migration of gastric cancer cells. In our previous research, we have found that HSG is related to the growth of rat C6 glioma cells, and exogenous HSG transcription can suppress the growth of C6 glioma cells [11, 12]. However, whether HSG can inhibit the invasion of human glioma cells has not been reported. The purpose of this study is to investigate the effect of HSG expression on the invasion of human glioma U251 cells and explore its possible mechanism by infecting human glioma U251 cells with a recombinant virus vector.

## Materials and methods

### *Main reagent*

Human glioma U251 cell lines were preserved at Cell Resource Center of Shanghai Academy of Biological Sciences, Chinese Academy of Sciences. Cell counting kit-8 was purchased from Japanese Dojindo, Recombinant viruses containing HSG gene sequence and green fluorescent protein gene sequence, negative control viruses and viral purified solutions containing HSG-RNAi interference sequence were purchased from Shanghai Jikai Gene Chemistry Technology Co., Ltd. Fetal bovine serum, DMEM culture medium, and PBS were purchased from HyClone Company, USA. Transwell chamber and Matrigel were purchased from Corning Company, USA. Penicillin-streptomycin mixture was purchased from Corning Company, USA. Hybrid solution and trypsin were purchased from Beijing Solebo Technology Co., Ltd. Ghost pencil cyclic peptide was purchased from AAT Bioquest Co., Ltd., USA. Real-time fluorescent quantitative PCR reagent was purchased from DBI Co., Germany. TRIzol and RNA reverse transcription reagent kit were purchased from Thermo Co., Ltd., USA. PCR primers were designed and synthesized by Bio-Biotechnology (Shanghai) Co., Ltd. Total protein extraction kit and BCA protein quantitative detection kit were purchased from Nanjing Kaiji Biotechnology Development Co., Ltd. Rabbit anti-human GAPDH polyclonal antibody was purchased from Wuhan Doude Bioengineering Co., Ltd. Rabbit anti-human HSG, Ras homolog gene family A (member A, RhoA), Ras-related C3 botulinum toxin substrate 1 (Rac1), Rho-related coil-forming protein kinase 1 (Rho associated coiled-coil forming protein kinase 1, Rock1) and Rock2 monoclonal antibodies, as well as rabbit anti-human cell division cycle 42 (Cdc42) polyclonal antibodies, were purchased from Abcam Company, USA. Goat anti-rabbit fluorescent antibody labeled with IRDye 800CW was purchased from LI-COR Company, USA. Crystal violet solution was purchased from Beijing Boaltoda Technology Co., Ltd. 4% polyarmor aldehyde fixatives were provided by Ningxia Key Laboratory of Craniocerebral Diseases, Ningxia Medical University.

### *Cell culture*

Human glioma U251 were cultured in DMEM complete culture medium containing 10% fetal bovine serum and 10 μl/ml penicillin-streptomycin mixture in an incubator with a volume fraction of 5% $CO_2$ tamping at 37°C. The cells in the logarithmic phase were digested with trypsin for 3 min, then digestion was stopped by adding DMEM complete culture medium. Then cells were disaggregated into single cell suspension by 3 ml pasteurized pipette for reserve.

### *Cell transcription and grouping*

The experiment was divided into four groups: PBS group (PBS), negative control group (NC), HSG overexpression group [(HSG+)], and HSG inhibition group [(HSG-)]. The density of U251 cell suspension was adjusted to $1\times10^6$/ml, and 300 μl/well were inoculated into a 6-well plate. After routine culture, the cells adhered to the wall and grew to 80% confluence. The serum-free DMEM culture medium was added to synchronize for 4 h, and then 10 μl virus purified solution was taken to infect U251 cells [multiplicity of transcription (MOI)=100]. Meanwhile, the same volume of PBS was used to intervene in U251 cells as the blank group. The medium was discarded and replaced with a DMEM complete culture medium containing 10% fetal bovine serum for further culture after 4 h of transcription.

### *Cell proliferation assay*

CCK-8 kit was used to detect cell proliferation. The U251 cells infected for 24 hours in each group were digested into a single cell suspension, and $5\times10^4$ cells/well were seeded in 96-well plate. Each group was set with 5 wells,

which were placed in 37°C and 5% $CO_2$ incubator for 30 hours. CCK-8 reagent was added into each well according to the instructions. The optical density (OD) value of each well at 450 nm was measured by enzyme labeling instrument.

*Wound healing assay*

The infected cells were inoculated into 6-well plates and cultured for 24 h. Scratches were made on the cell surface with a sterilized 200 μl pipette tip. Then we added medium after washing the cell surface with the PBS (marked as 0 h). The cells were observed and photographed by Nikon Eclipse Ti-S inverted fluorescence microscope (10×20 times), and the scratch width was measured by NIS-Elements D 3.2 software. Three visual fields were randomly selected for each well, and three different sites were randomly measured for each eye, and the average was taken as scratch width. After 30 h of culture, the scratch width of cells in each group was measured by the same method. According to the difference of the width of the second scratch, the mobility was calculated to reflect the migration ability of each group of cells. Mobility (%)=(0 h scribe width - 30 h scribe width)/0 h scribe width ×100%.

*Migration and invasion assay*

Matrigel was diluted with a DMEM medium at a volume ratio of 1:5 and evenly coated on the transwell chamber membrane (24 holes, pore size 8 microns). The transwell chamber was placed in a 37°C thermostat for 30-60 min to solidify the gel. Then a suitable amount of DMEM medium containing 20% FBS was added into the transwell chamber. At the same time, U251 cells of each group were collected after 24 h of virus transcription, and the cell density was adjusted to $1\times10^5$ cells/ml. 100 μl per well was inoculated into the upper chamber. Each group had three multiple wells. DMEM medium containing 5% FBS was added into the upper chamber, and incubated for 24 h in a constant temperature incubator with 37°C and 5% $CO_2$ volume fraction. Using a cotton swab we gently wiped the cells of the upper chamber which did not pass through the membrane, and the transwell chamber was taken out and cleaned with PBS for three times. Cells were fixed in methanol solution for 10 min and washed with PBS for 3 times, then stained with 0.1% crystal violet solution for 20 min and washed with PBS for 3 times. The number of cells passing through the membrane was observed under an inverted microscope (10×20 times). Three visual fields were randomly counted in each well, and the average number was taken to reflect the invasive ability of cells in each group.

Cell migration ability was detected by the same method. Instead of Matrigel coating, three groups of cell suspensions were directly inoculated into the upper chamber after virus transcription. The subsequent steps and counting methods were the same as cell invasion experiments.

*Cell Adhesion assay*

Matrigel was diluted with DMEM medium at a ratio of 1:5 and evenly coated on 96-well plate with 20 μl per hole. After drying overnight, cells were washed twice with PBS to remove unsolidified excess glue. U251 cells of each group were collected after virus transcription for 48 h and inoculated into a 96-well plate with a density of 4000 cells per well. Each group had three multiple well, which were cultured in a constant temperature incubator with a volume fraction of 5% $CO_2$ at 37°C. At 30, 60, 90, and 120 min, the culture medium was removed and cleaned with PBS twice. The cells were fixed in 95% methanol solution for 10 min and washed twice with PBS. Cells were stained with 0.1% crystal violet for 20 min and washed with PBS for three times; the cells were observed and photographed under an inverted microscope (10×20 times). Five visual fields were randomly taken to count the number of adherent cells per well, and the average number of adherent cells was taken to reflect the cell adhesion ability.

*Immunofluorescence assay*

U251 cells of each group were collected after 24 h of virus transcription, digested into single cell suspension with trypsin, and the cell density was adjusted to $1\times10^5$ cells/ml. The cells were inoculated into a 24 - well plate with 500 ml per well for 24 h, and then cultured for 24 h to make cell slides. Cells were washed twice with PBS, and fixed with 4% polyformaldehyde solution for 10 min. Then the cells were washed with PBS for three times and stained

with ghost pencil ring peptide (according to the instructions of reagents). After washing with PBS, the cells was sealed by using neutral gum and the cytoskeleton was observed under a confocal laser microscope (2000 times).

*Gene chip assay*

U251 cells of HSG overexpression group and HSG inhibition group were collected 24 h after virus transcription. Total RNA was extracted by Trizol method. Qualified samples were examined by NanoDrop 2000 and Agilent Bioanalyzer 2100. The chip experiment was carried out with the help of Shanghai Jikai Gene Chemistry Technology Co., Ltd.

*RT-PCR assay*

Each group of U251 cells infected with virus for 48 h was collected. RNA was extracted by TRIzol method, and the concentration was determined by Thermo NanoDrop 2000 spectrophotometer. RNA was re-transcribed according to the instructions of the reverse transcription kit to synthesize the cDNA. cDNA was used as a template, and three-step PCR amplification was carried out on BIO-RAD fluorescence quantitative PCR instrument according to the instructions of real-time fluorescence quantitative PCR reagent. The upstream primer sequence of the RhoA gene was 5'-TGGATGGAAAGCAGGTAGAGT-3', downstream primer sequence was 5'-GTTGGGACAGAAATGCTTGAC-3'. The upstream primer sequence of Rock1 gene was 5'-CTTTTGGACCTCTCGGATTCTA-3', downstream primer sequence was 5'-GGATTGCTCCTTATCTTGTTCG-3'. The upstream primer sequence of Rock2 gene was 5'-TGA CAT TGG ACA GTA AAG ACA GTG-3', downstream primer sequence was 5'-AGT GTT GTT TCG TAC AGG CAA T-3'. The upstream primer sequence of Rac1 gene was 5'-TACAGCACCAATCTCCTTA-3', downstream primer sequence was 5'-CCCAACACTCCCATCAT-3'. The upstream primer sequence of Cdc42 gene was 5'-AGTCTAGAGCCACCGTCCAC-3', downstream primer sequence was 5'-TCTGACGCACACCTATTGCAA-3'. The upstream primer sequence of HSG was 5'-GTGCCAAGACTGTGAACCAG-3', downstream primer sequence was 5'-TGTCCATCAAAACGAGGTCA-3'. A total of 20 μl of PCR reaction system was established, including 2 μl of DNA, 1 μl of upstream and downstream primers, 10 μl of real-time fluorescent quantitative PCR reagent and 6 μl of sterile ultra-pure water. The conditions of PCR reaction were as follows: pre-denaturation at 95°C for 2 min; 40 cycles at 95°C for 10 s, 60 33 s, 72 30 s. The reaction conditions for plotting the melting curve were 95°C for 1 min and 55°C for 1 min. The relative expression level of the target gene was calculated by the $2^{-\Delta\Delta CT}$ method.

*Western blotting assay*

U251 cells in each group were infected by the virus for 48 h. The cells were lysed with an appropriate amount of lysate solution. The total protein was extracted and the concentration of protein was determined. Then the protein was denatured by adding sample buffer at 100°C for 5 min. SDS-PAGE (90 V, 90 min) was used to isolate the protein from 50 mg protein (25 μl) and then electrophoresis membrane (300 mA, 70 min) and the PVDF membrane was sealed with skimmed milk for 1 h. Rabbit anti-human GAPDH and CD42 polyclonal antibodies and rabbit anti-human HSG, RhoA, Rock1, Rock2 and Rac1 monoclonal antibodies were added respectively (the volume dilution ratio was 1:1000), and TBS buffer was used to wash the membrane overnight. Afterward, the goat anti-rabbit fluorescent antibody labeled with IRDye 800CW (the volume dilution ratio is 1:4000) was used to hybridize at room temperature for 1 h. After the film was washed again, it was exposed by the Odyssey Infrared Imaging instrument. The gray value of the protein bands was scanned by ImageJ Setup software, and the relative expression level of each protein was expressed by the ratio of the gray value of the target protein to the internal reference GAPDH protein bands.

*Statistical method*

SPSS 17.0 and GraphPad Prism 5 statistical software were used to analyze the experimental data. All the experiments were repeated three times independently, and the results were expressed as $\bar{x} \pm s$. Means were compared among groups by one-way ANOVA, and the LSD-t test was used for intra-group comparisons. The difference was significant if $P < 0.05$. Fisher's Exact Test was used for gene chip pathway enrichment analysis.

## Results

*HSG inhibiting glioma cell proliferation*

The OD value of PBS group, negative control group, HSG overexpression group, and HSG

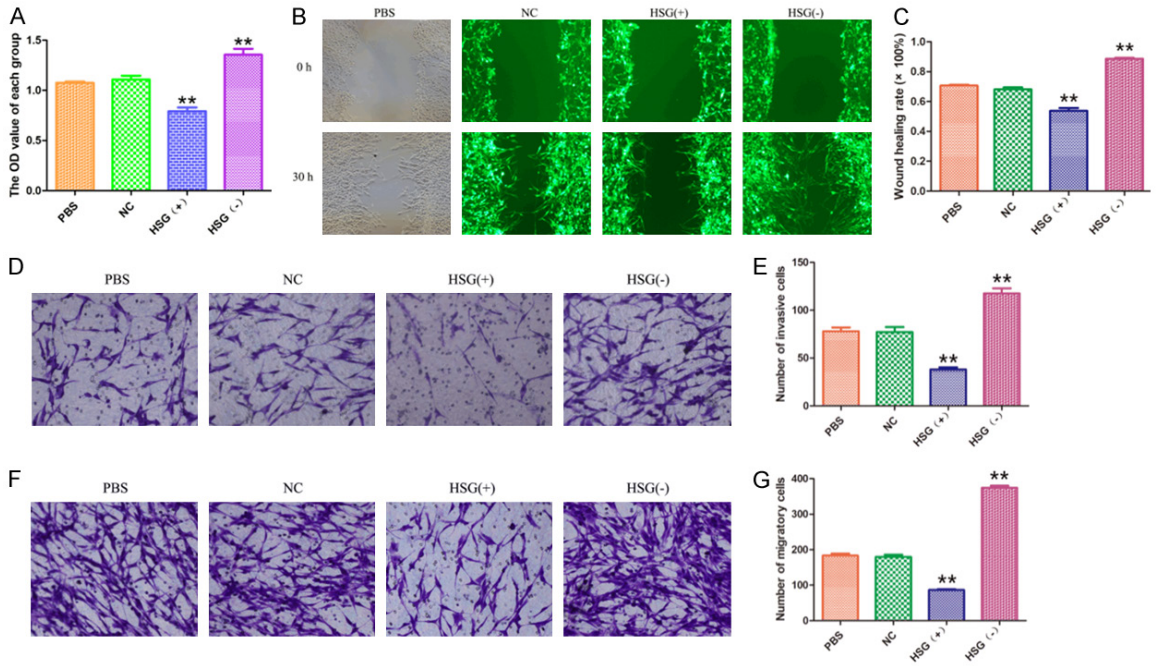


**Figure 1.** The proliferation (A), wound healing rates (B, C), migration (F, G) and invasion (D, E) of U251 cells in each group (**P < 0.01, n=3). PBS group (PBS), negative control group (NC), HSG overexpression group [(HSG+)], and HSG inhibition group [(HSG-)]. Compared with the two control groups, the healing rate as well as the numbers of proliferative, migratory and invasive cells in HSG overexpression group were significantly decreased, but the healing rate, the numbers of proliferative, migratory and invasive cells in HSG inhibition group were significantly increased.

infection group were (1.08±0.02), (1.10±0.04), (0.79±0.04), (1.36±0.06) after 30 hours of culture (**Figure 1A**). There was no significant difference between PBS group and negative control group ($P > 0.05$, **Figure 1A**). Compared with the PBS group and negative control group, the OD value of HSG overexpression group decreased ($P < 0.05$, **Figure 1A**), and the OD value of HSG infection group increased ($P < 0.05$, **Figure 1A**). This suggests that the change of HSG affects the proliferation of U251 glioma cells. Overexpression of HSG inhibited the proliferation of U251 glioma cells.

*HSG inhibits glioma cell migration rate in cell wound healing assay*

The green fluorescence expression in U251 glioma cells was high after infecting with the virus for 24 h with the changing of the expression of the mRNA and proteins of HSG accordingly at the same time, indicating the success of the virus transfection (**Figure 1B**). The results of cell scratch healing experiment showed that the cell migration rates of PBS group, negative control group, HSG overexpression group and HSG inhibition group were (71.7±2.0)%, (68.1±4.0)%, (53.8±5.7)% and (89.7±2.0)% after 30 h of scratch healing (**Figure 1C**). There were significant differences between the groups (F= 132.30, $P < 0.01$, **Figure 1C**). Compared with the PBS group and negative control group, the cell migration rates of HSG overexpression group were significantly lower ($P < 0.01$, **Figure 1C**). The cell migration rate in HSG inhibition group was significantly higher than that in PBS group ($P < 0.01$, **Figure 1C**), but there was no significant difference between PBS group and negative control group ($P > 0.05$, **Figure 1C**). These results suggested that HSG overexpression inhibits glioma cell migration.

*HSG suppresses glioma cell invasion in transwell assay*

The transwell migration assay (**Figure 1F**) showed that the average number of cells in PBS group, negative control group, HSG overexpression group, and HSG inhibition group migrated to each goal under ventricular filter membrane were (183.5±13.84), (179.67±15.44), (86.5±5.89) and (374.8±13.61). Significant differences were observed between the groups (F= 541.49, $P < 0.01$, **Figure 1G**). Compared with the PBS group and negative control group, the

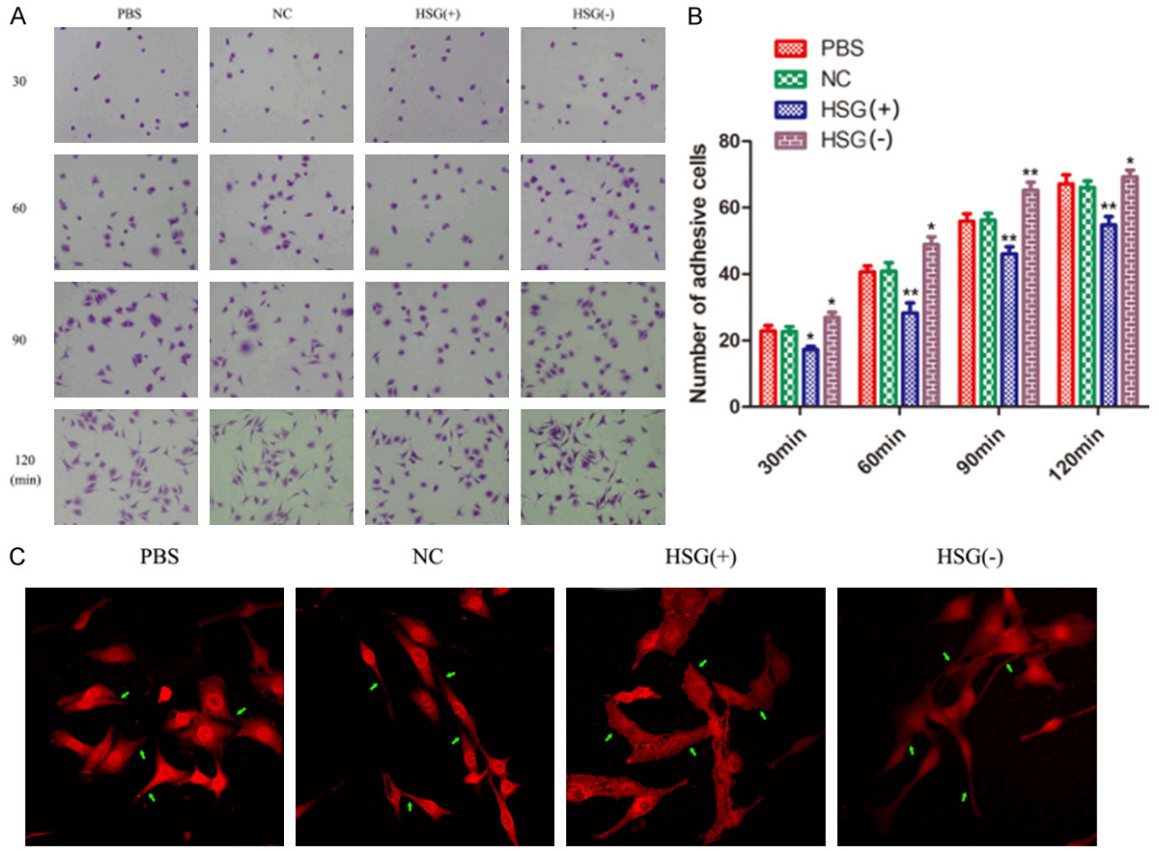


**Figure 2.** The adhesion ability (A, B) and cytoskeleton (C) of U251 cells in different groups (*P < 0.05, **P < 0.01, n=3). Compared with the two control groups, the number of adhesion cells in HSG overexpression group was significantly decreased, And the morphology of U251 cells changed, showing filopodia shortening or some lamellipodia, but the number of adhesion cells in HSG overexpression group was significantly increased, and the morphology of U251 cells did not change.

number of migrating cells decreased sharply in the HSG overexpression group ($P < 0.01$, **Figure 1G**), but increased remarkably in the HSG inhibition group ($P < 0.01$, **Figure 1G**). No significant difference was found between the PBS group and negative group ($P > 0.05$, **Figure 1G**).

From the results of transwell invasion assay (**Figure 1D**), the average number of cells in PBS group, negative control group, HSG overexpression group, and HSG inhibition group invaded into each visual area under ventricular filter membrane were (78.00±9.84), (77.33±12.37), (38.00±5.73) and (117.67±12.80), respectively. There were significant differences between the groups (F=56.86, $P < 0.01$, **Figure 1E**). Compared with the PBS group and negative group. The number of invasive cells significantly decreased in the HSG overexpression group ($P < 0.01$, **Figure 1E**), but increased in the HSG inhibition group ($P < 0.01$, **Figure 1E**). However, there was no significant difference between the PBS group and negative control group ($P > 0.05$, **Figure 1E**).

The results of this study indicated that the proliferation, migration, and invasiveness of U251 glioma cells were significantly inhibited after HSG overexpression, but relatively enhanced after the HSG inhibition.

*HSG attenuates cell adhesion ability of glioma cells*

The number of adherent cells increased gradually with time, and the cells gradually extended pseudopodia from a spherical shape. The longer the adhesion time was, the more obvious the pseudopodia appeared (**Figure 2A**). At different time points (30, 60, 90 and 120 min), there were significant differences among the four groups (F value was 7.58, 12.18, 12.79 and 8.00, $P < 0.01$, **Figure 2B**), and the number of adherent cells in the HSG overexpression

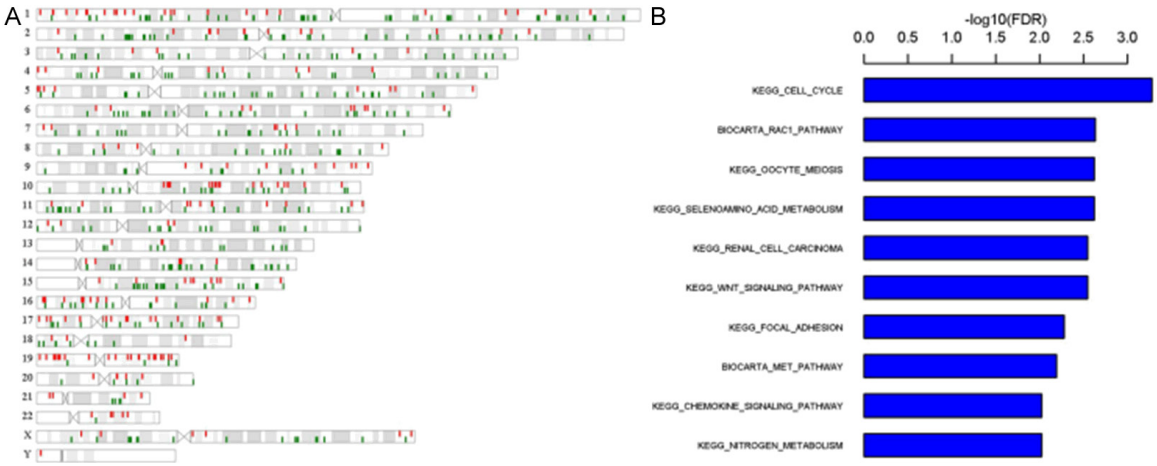


**Figure 3.** Differentially expressed genes in the HSG inhibition group and HSG overexpression group. HSG is closely related with cell proliferation, apoptosis, migration signal Approaches.

group was significantly reduced compared with the other three groups. The degree of reduction was gradually reduced with time ($P < 0.05$ at 30 min, $P < 0.01$ at 60, 90, and 120 min, **Figure 2B**). The number of adherent cells in the HSG inhibition group was higher than that in the other three groups, and the degree of increase gradually decreased with time prolongation ($P < 0.05$ at 30 and 60 min, $P < 0.01$ at 90 min and $P < 0.05$ at 120 min, **Figure 2B**). There was no significant difference between the PBS group and negative control group ($P > 0.05$, **Figure 2B**). The results revealed that the adhesion ability of U251 glioma cells was significantly inhibited after HSG overexpression. The adhesion ability of U251 glioma cells was relatively enhanced after HSG inhibition. However, with the prolongation of the adhesion time, the effect of HSG on the adhesion of U251 glioma cells was gradually reduced.

*HSG interferes with the formation of the glioma cell skeleton*

Immunofluorescence was performed to analyze the formation of the cytoskeleton in U251 glioma cells. The cells in the PBS group and negative control group were mostly spindle-shaped or star-shaped, with more axons extending. Some of them had linear or filamentous pseudopodia, and the pseudopodia stretched to two ends in an axial direction. In the HSG overexpression group, the axons of U251 glioma cells were retracted, patchy, and some cells were irregular and disorderly arranged. In the HSG inhibition group, U251 glioma cells were similar to those in the PBS group and negative group, and cells were mostly spindle-shaped or star-shaped, with pseudopods growing toward both ends and arranged axially (**Figure 2C**). The above results showed that the change of HSG expression had some effects on the cytoskeleton of U251 cells. Overexpression of HSG suppressed the formation of the cytoskeleton of U251 cells.

*Variations in gene expression profile after HSG alteration*

Bioinformatic analysis was conducted based on the gene chip data. The difference in gene expression between the HSG overexpression group and the HSG suppression group was assessed. At $P < 0.05$, the number of differentially expressed genes was 2214. FC > 1.5 was used to further narrow the screening range, and the number of differentially expressed genes was 656, in which the number of up-regulated genes was 217 and the down-regulated genes was 439. Referring to the KEGG and BioCarta databases, pathway enrichment analysis was adopted to identify the metabolic and signal transduction pathways that were obviously affected, most of which were tumor related genes involving in the cell cycle, meiosis, cell invasion and adhesion adhesion (**Figure 3A**, **3B**).

*HSG overexpression impacts the mRNA levels of Rho family key molecules*

RT-PCR results showed that the expression of Rho family key molecules RhoA, Rock1, Rock2, Rac1 and Cdc42 in U251 glioma cells decreased when HSG was overexpressed (**Figure 4A**). There were significant differences between the

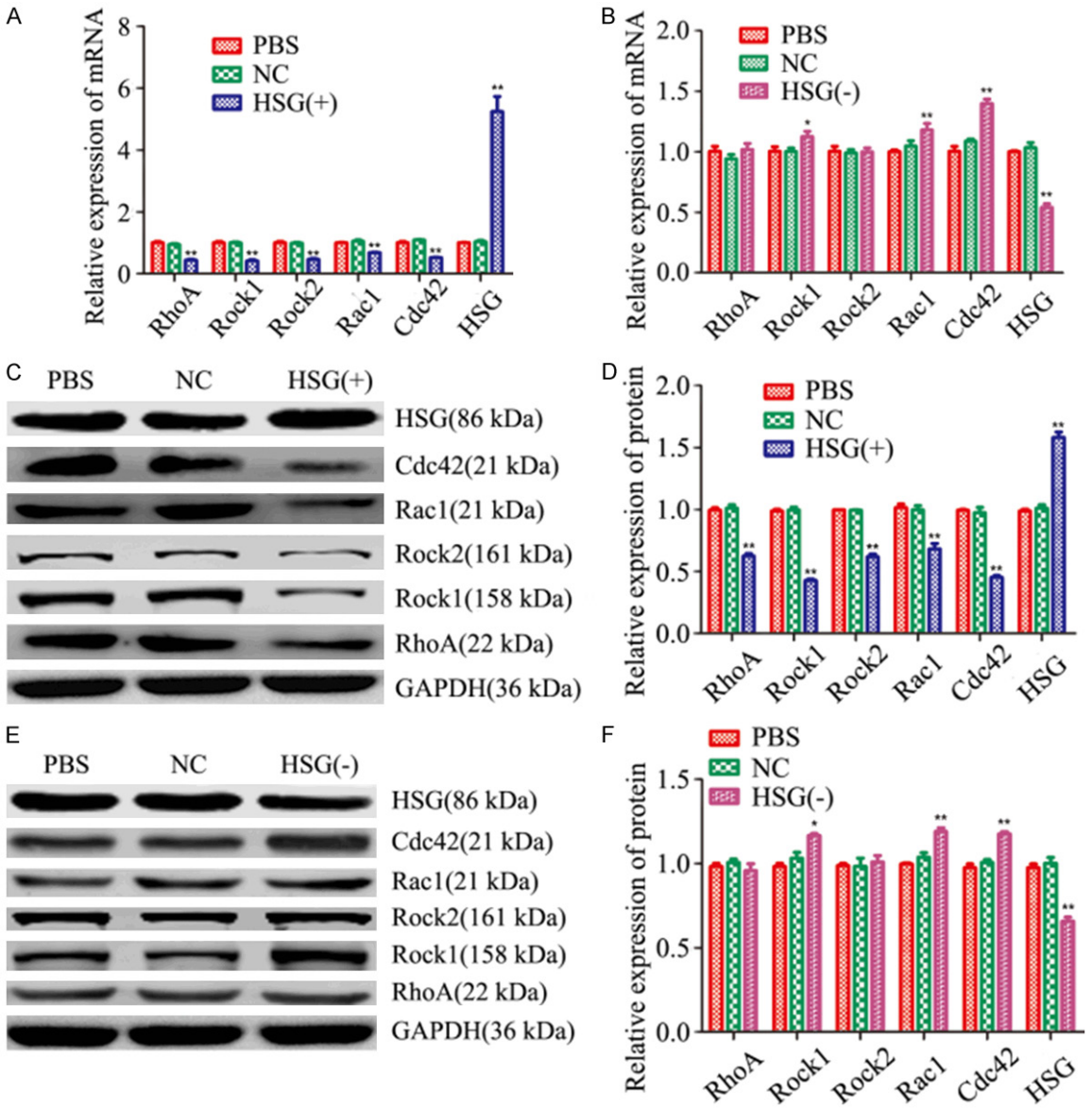


**Figure 4.** RT-PCR (A, B) analysis of HSG and Rho family key molecules in U251 cells; western blot (C-F) analysis of HSG and Rho family key molecules in U251 cells (*P < 0.05, **P < 0.01, n=3). RhoA: Ras homolog gene family, member A; Rac1: Ras-related C3 botulinum toxin substrate 1; Cdc42: Cell division cycle 42; Rock1/2: Rho associated coiled-coil forming protein kinase 1/2. The results showed that when the expression of HSG was up-regulated in U251 cells, the expressions of RhoA, Rac1, Cdc42, Rock1 and Rock2 were significantly decreased. When the expression of HSG was down-regulated in U251 cells, the expressions of Rac1, Cdc42 and Rock1 were significantly increased, but RhoA and Rock2 did not change.

HSG overexpression group and the blank control group/negative control group (F values were 37.23, 63.84, 41.22, 33.77, 74.94, $P < 0.01$, **Figure 4A**). Compared to the blank control group and negative control group, the expression of RhoA and Rock2 had no significant change in HSG inhibition group ($P > 0.05$, **Figure 4B**), while the expression of Rock1, Rac1, and Cdc42 increased [F value was 27.14, 45.37, 36.08, $P < 0.05$ (Rock1), $P < 0.01$ (Rac1, Cdc42), **Figure 4B**]. In addition, the expression of each molecule in the blank control group was lower than that in negative control group. No difference was observed between the expression groups ($P > 0.05$, **Figure 4B**).

*HSG overexpression results in altered expression of Rho family key molecules in protein levels*

According to the western blotting results (**Figure 4C**, **4E**), the expression of Rho family key mole-

cules RhoA, Rock1, Rock2, Rac1, and Cdc42 in U251 glioma cells decreased when HSG was overexpressed (**Figure 4D**). There were significant differences between the HSG overexpression group, and the blank control group and the negative control group (F values were 91.05, 391.80, 284.00, 27.48, 129.13, $P < 0.01$, **Figure 4D**). Compared with the blank control group and the negative control group, the expression of RhoA and Rock2 in the HSG inhibition group had no marked change ($P > 0.05$, **Figure 4F**), while the expression of Rock1, Rac1, and Cdc42 was increased (F value was 15.60, 24.77, 35.65, $P < 0.05$ (Rock1), $P < 0.01$ (Rac1 and Cdc42), **Figure 4F**). The blank control group and negative control group were not significantly different ($P > 0.05$, **Figure 4E**, **4F**).

## Discussion

Recent evidence suggests that the abnormal expression of HSG is related to many kinds of tumor growth, and its overexpression has a significant antitumor effect. In this study, human glioma U251 cells were cultured in vitro based on the previous experiments. HSG expression was artificially interfered with by the virus vector in cells. Scratch healing test, transwell migration, and invasion test showed that the overexpression of HSG significantly inhibited the migration and invasion of glioma cells. The migration and invasion of U251 cells was relatively enhanced after the HSG expression was inhibited, which was similar to the study results in gastric cancer by Zhang et al. [9]. The findings in the adhesion test indicated that the overexpression of HSG could significantly reduce the adhesion of glioma cells to the extracellular matrix, further suggesting that HSG had a relationship to the invasion of glioma. Moreover, the results of the immunofluorescence assay showed that the overexpression of HSG caused some glioma cells to change in morphology, showing that the numerous filopodia were shortened or lamellipodium was arranged disorderly. Some cells changed from fusiform to sphericity. But the cells were mostly in spindle shape with the pseudopods were arranged axially at both ends when the expression of HSG decreased. Besides, the preliminary results of gene chip experiments showed the changing of HSG expression profiles involving in the signal pathways of tumor migration, invasion, adhesion and cell cycle. Real-time fluorescence quantitative PCR and western blotting were used to detect the expression of Rho family related molecules RhoA, Rock1, Rock2, Rac1 and Cdc42 in U251 cells. On average, the expression of these molecules decreased when HSG expression was increased, but increased partially when HSG expression was inhibited. Rho family molecules are known to promote the movement and invasion of cancer cells by regulating cytoskeletal reorganization [13, 14]. Therefore, it is assumed that HSG can inhibit the invasiveness of human glioma U251 cells, and the underlying mechanism may be related to suppressing the expression of Rho family molecules, thereby affecting the recombination of glioma cytoskeleton.

Rho family belongs to a subfamily of Ras superfamily. It exists widely in mammals and is the most well-known Ras-related monomer GTPase. The key molecules of the Rho/Rock signal transduction pathway include Rho family molecules, Rock and myosin phosphatase [13]. Members of the Rho GTPase family, including RhoA, Rac, and Cdc42, are key regulators of cell migration by modulating mesenchymal and amoeboid motility [14, 15]. Rac is required for the formation of actin-rich membrane ruffles, called lamellipodia, at the leading edge of the migrating cells, whereas RhoA regulates the formation of contractile actin-myosin filaments, which form stress fibers, and maintains focal adhesion at the lagging edge of the cells [16-18].

Several reports suggest RhoA/Rock are ideal therapeutic targets to fight metastasis and invasion of glioma [19, 20]. In GBM, the differential expression of RhoGTPase family members dictates invasive strategies [21]. Rho GTPases are molecular switches that mediate their effects through interactions with downstream effectors [22]. RhoA, Rac1 and Cdc42 are three widely studied members of the Rho family. Each member plays an independent and important role in cell adhesion, cytoskeleton formation, cell movement, and invasion and metastasis of malignant tumors [23-25]. It has been proven that the Rho family is closely related to the invasion and malignancy of glioma. The expression level of RhoA increases in high-grade glioma, and the decrease of the RhoA expression or activity directly weakens the invasive ability of glioma cells [13, 26]. The expression level of Rac1 increased with the grade of glioma. Rac1 protein mainly exists on the sur-

face of the prominent plasma membrane in glioma cells and plays an vital role in the activity of glioma cells [27]. Additionally, Rac1 activation can promote malignant transformation and progression of tumors and enhance the invasiveness of tumors. In glioma cells, inhibition of Rac1 activity can hamper cell invasion. Downregulation of Rac1 expression can restrain the characteristics of glioma stem cells, such as suppress of neurosphere formation and expression of self-repair related proteins [28]. Cdc42 is a molecule closely related to actin cytoskeleton recombination, cell migration, and adhesion, especially the regulation of cell polarity [29]. In other cancer cell systems, it has been shown that the active form of Cdc42 is able to increase cancer migration and carcinogenesis [30, 31]. The suppression of Cdc42 activity can lead to a decrease in glioma invasion and migration [32]. At the same time, some studies have shown that Cdc42 is the upstream molecule of Rac1, that is, Cdc42 can activate Rac1; therefore, by inhibiting the expression and activation of Cdc42, it can hinder the movement and invasion of glioma cells [27].

Rock proteins, belonging to the serine/threonine protein kinases, include Rock1 and Rock2 subtypes. Rock proteins are the typical downstream effector molecules of RhoA in glioma, and also the most well-known target effector molecules of the RhoA family. The inhibition of Rock expression can interfere with the formation of the actin skeleton structure mediated by Rho in most cases, which participates in cell movement and tumor progression [33-35].

Findings suggest that Rho family proteins are essential for the invasion of glioma cells, which further supports the above conclusions. In sum, HSG can inhibit the invasion of glioma cells by regulating the expression of Rho family proteins. The results of this study provide a new experimental basis for further elucidating the anti-glioma effect of HSG, and lay a foundation for the follow-up study of new strategies and drug development for HSG treatment of glioma.

## Acknowledgements

The present study was supported by the Ningxia Natural Science Foundation (grant no. 2018AAC03271).

## Disclosure of conflict of interest

None.

**Address correspondence to:** Juncheng Wang, Department of Neurosurgery, People's Hospital of Ningxia Hui Autonomous Region, 301 Zhengyuan North Street, Jinfeng District, Yinchuan 750001, Ningxia Hui Autonomous Region, China. E-mail: Drwangjc919@163.com

## References

[1] Galanis E, Anderson SK, Twohy EL, Carrero XW, Dixon JG, Tran DD, Jeyapalan SA, Anderson DM, Kaufmann TJ, Feathers RW, Giannini C, Buckner JC, Anastasiadis PZ and Schiff D. A phase 1 and randomized, placebo-controlled phase 2 trial of bevacizumab plus dasatinib in patients with recurrent glioblastoma: Alliance/North Central Cancer Treatment Group N0872. Cancer 2019; 125: 3790-3800.

[2] Caragher SP, Shireman JM, Huang M, Miska J, Atashi F, Baisiwala S, Hong PC, Saathoff MR, Warnke L, Xiao T, Lesniak MS, James CD, Meltzer H, Tryba AK and Ahmed AU. Activation of dopamine receptor 2 prompts transcriptomic and metabolic plasticity in glioblastoma. J Neurosci 2019; 39: 1982-1993.

[3] Catacuzzeno L, Caramia M, Sforna L, Belia S, Guglielmi L, D'Adamo MC, Pessia M and Franciolini F. Reconciling the discrepancies on the involvement of large-conductance Ca(2+)-activated K channels in glioblastoma cell migration. Front Cell Neurosci 2015; 9: 152.

[4] Hayashi K, Michiue H, Yamada H, Takata K, Nakayama H, Wei FY, Fujimura A, Tazawa H, Asai A, Ogo N, Miyachi H, Nishiki T, Tomizawa K, Takei K and Matsui H. Fluvoxamine, an antidepressant, inhibits human glioblastoma invasion by disrupting actin polymerization. Sci Rep 2016; 6: 23372.

[5] Joseph JV, van Roosmalen IA, Busschers E, Tomar T, Conroy S, Eggens-Meijer E, Penaranda FN, Pore MM, Balasubramanyian V, Wagemakers M, Copray S, den Dunnen WF and Kruyt FA. Serum-induced differentiation of glioblastoma neurospheres leads to enhanced Migration/Invasion capacity that is associated with increased MMP9. PLoS One 2015; 10: e0145393.

[6] Chen KH, Guo X, Ma D, Guo Y, Li Q, Yang D, Li P, Qiu X, Wen S, Xiao RP and Tang J. Dysregulation of HSG triggers vascular proliferative disorders. Nat Cell Biol 2004; 6: 872-83.

[7] Wang W, Lu J, Zhu F, Wei J, Jia C, Zhang Y, Zhou L, Xie H and Zheng S. Pro-apoptotic and antiproliferative effects of mitofusin-2 via Bax signaling in hepatocellular carcinoma cells. Med Oncol 2012; 29: 70-6.

[8] Jin B, Fu G, Pan H, Cheng X, Zhou L, Lv J, Chen G and Zheng S. Anti-tumour efficacy of mitofusin-2 in urinary bladder carcinoma. Med Oncol 2011; 28 Suppl 1: S373-80.

[9] Wu L, Li Z, Zhang Y, Zhang P, Zhu X, Huang J, Ma T, Lu T, Song Q, Li Q, Guo Y, Tang J, Ma D, Chen KH and Qiu X. Adenovirus-expressed human hyperplasia suppressor gene induces apoptosis in cancer cells. Mol Cancer Ther 2008; 7: 222-32.
[10] Zhang GE, Jin HL, Lin XK, Chen C, Liu XS, Zhang Q and Yu JR. Anti-tumor effects of Mfn2 in gastric cancer. Int J Mol Sci 2013; 14: 13005-21.
[11] Gao P, Zou Y, Zhang B, Jiang S, Hao W, Guo H, Huo G, Wang J, Zhao W and Shen B. Pro-apoptotic effects of rHSG on C6 glioma cells. Int J Mol Med 2016; 38: 1190-8.
[12] Gao P, Wang Z, Zhang B, Zou Y, Guo H, Liu H, Yang Q, Fang Z, Jiang S, Shen B, Chow LW, Loo WT, Ng EL and Tsang WW. Suppression of C6 gliomas via application of rat hyperplasia gene. Int J Biol Markers 2014; 29: e411-22.
[13] Zohrabian VM, Forzani B, Chau Z, Murali R and Jhanwar-Uniyal M. Rho/ROCK and MAPK signaling pathways are involved in glioblastoma cell migration and proliferation. Anticancer Res 2009; 29: 119-23.
[14] Hara A, Hashimura M, Tsutsumi K, Akiya M, Inukai M, Ohta Y and Saegusa M. The role of FilGAP, a Rac-specific Rho-GTPase-activating protein, in tumor progression and behavior of astrocytomas. Cancer Med 2016; 5: 3412-3425.
[15] Raftopoulou M and Hall A. Cell migration: Rho GTPases lead the way. Dev Biol 2004; 265: 23-32.
[16] Ridley AJ. Rho proteins and cancer. Breast Cancer Res Treat 2004; 84: 13-9.
[17] Sahai E and Marshall CJ. RHO-GTPases and cancer. Nat Rev Cancer 2002; 2: 133-42.
[18] Schmitz AA, Govek EE, Bottner B and Van Aelst L. Rho GTPases: signaling, migration, and invasion. Exp Cell Res 2000; 261: 1-12.
[19] Deng B, Liu R, Tian X, Han Z and Chen J. Simulated microgravity inhibits the viability and migration of glioma via FAK/RhoA/Rock and FAK/Nek2 signaling. In Vitro Cell Dev Biol Anim 2019; 55: 260-271.
[20] Liu H, Liu B, Hou X, Pang B, Guo P, Jiang W, Ding Q, Zhang R, Xin T, Guo H, Xu S and Pang Q. Overexpression of NIMA-related kinase 2 is associated with poor prognoses in malignant glioma. J Neurooncol 2017; 132:409-417.
[21] Hirata E, Yukinaga H, Kamioka Y, Arakawa Y, Miyamoto S, Okada T, Sahai E and Matsuda M. In vivo fluorescence resonance energy transfer imaging reveals differential activation of Rho-family GTPases in glioblastoma cell invasion. J Cell Sci 2012; 125: 858-68.
[22] Pettee KM, Becker KN, Alberts AS, Reinard KA, Schroeder JL and Eisenmann KM. Targeting the mDia Formin-Assembled cytoskeleton is an effective anti-invasion strategy in adult High-Grade glioma patient-derived neurospheres. Cancers (Basel) 2019; 11: 392.
[23] Yu G, Wang Z, Zeng S, Liu S, Zhu C, Xu R and Liu RE. Paeoniflorin inhibits hepatocyte growth factor- (HGF-) induced migration and invasion and actin rearrangement via suppression of c-Met-Mediated RhoA/ROCK signaling in glioblastoma. Biomed Res Int 2019; 2019: 9053295.
[24] Liu Z, Adams HR and Whitehead IP. The rho-specific guanine nucleotide exchange factor Dbs regulates breast cancer cell migration. J Biol Chem 2009; 284: 15771-80.
[25] Infante E and Ridley AJ. Roles of Rho GTPases in leucocyte and leukaemia cell transendothelial migration. Philos Trans R Soc Lond B Biol Sci 2013; 368: 20130013.
[26] Tong JJ, Yan Z, Jian R, Tao H, Hui OT and Jian C. RhoA regulates invasion of glioma cells via the c-Jun NH2-terminal kinase pathway under hypoxia. Oncol Lett 2012; 4: 495-500.
[27] Fortin SP, Ennis MJ, Schumacher CA, Zylstra-Diegel CR, Williams BO, Ross JT, Winkles JA, Loftus JC, Symons MH and Tran NL. Cdc42 and the guanine nucleotide exchange factors Ect2 and trio mediate Fn14-induced migration and invasion of glioblastoma cells. Mol Cancer Res 2012; 10: 958-68.
[28] Karpel-Massler G, Westhoff MA, Zhou S, Nonnenmacher L, Dwucet A, Kast RE, Bachem MG, Wirtz CR, Debatin KM and Halatsch ME. Combined inhibition of HER1/EGFR and RAC1 results in a synergistic antiproliferative effect on established and primary cultured human glioblastoma cells. Mol Cancer Ther 2013; 12: 1783-95.
[29] Senini V, Amara U, Paul M and Kim H. Porphyromonas gingivalis lipopolysaccharide activates platelet Cdc42 and promotes platelet spreading and thrombosis. J Periodontol 2019; 90: 1336-1345.
[30] Briggs MW and Sacks DB. IQGAP proteins are integral components of cytoskeletal regulation. EMBO Rep 2003; 4: 571-4.
[31] Choi S, Thapa N, Hedman AC, Li Z, Sacks DB and Anderson RA. IQGAP1 is a novel phosphatidylinositol 4,5 bisphosphate effector in regulation of directional cell migration. EMBO J 2013; 32: 2617-30.
[32] Okura H, Golbourn BJ, Shahzad U, Agnihotri S, Sabha N, Krieger JR, Figueiredo CA, Chalil A, Landon-Brace N, Riemenschneider A, Arai H, Smith CA, Xu S, Kaluz S, Marcus AI, Van Meir EG and Rutka JT. A role for activated Cdc42 in glioblastoma multiforme invasion. Oncotarget 2016; 7: 56958-56975.
[33] Mertsch S and Thanos S. Opposing signaling of ROCK1 and ROCK2 determines the switching of substrate specificity and the mode of migration of glioblastoma cells. Mol Neurobiol 2014; 49: 900-15.

[34] Ishizaki T, Naito M, Fujisawa K, Maekawa M, Watanabe N, Saito Y and Narumiya S. P160ROCK, a Rho-associated coiled-coil forming protein kinase, works downstream of Rho and induces focal adhesions. FEBS Lett 1997; 404: 118-24.

[35] O'Connor K and Chen M. Dynamic functions of RhoA in tumor cell migration and invasion. Small GTPases 2013; 4: 141-7.